Kinetic Analysis of Oligodeoxyribonucleotide-Directed Triple-Helix Formation on DNA†

L. James Maher, III, Peter B. Dervan, and Barbara J. Wold*

Divisions of Biology and of Chemistry and Chemical Engineering, California Institute of Technology, Pasadena, California 91125

Received March 21, 1990; Revised Manuscript Received May 25, 1990

ABSTRACT: Pyrimidine oligonucleotides recognize extended purine sequences in the major groove of double-helical DNA by triple-helix formation. The resulting local triple helices are relatively stable and can block DNA recognition by sequence-specific DNA binding proteins such as restriction endonucleases. Association and dissociation kinetics for the oligodeoxyribonucleotide 5′-CTCTTTCCTCTCTTTTTCCCC (bold C's indicate 5-methylcytosine residues) are now measured with a restriction endonuclease protection assay. When oligonucleotides are present in >10-fold excess over the DNA target site, the binding reaction kinetics are pseudo first order in oligonucleotide concentration. Under our standard conditions (37 °C, 25 mM Tris–acetate, pH 6.8, 70 mM sodium chloride, 20 mM magnesium chloride, 0.4 mM spermine tetrahydrochloride, 10 mM β-mercaptoethanol, 0.1 mg/mL bovine serum albumin) the value of the observed pseudo-first-order association rate constant, k_{2obs}, is $1.8 \times 10^3 \pm 1.9 \times 10^2$ L·(mol of oligomer)$^{-1}$·s^{-1}. Measurement of the dissociation rate constant yields an equilibrium dissociation constant of approximately 10 nM. Increasing sodium ion concentration slightly decreased the association rate, substantially increased the dissociation rate, and thereby reduced the equilibrium binding constant. This effect was reversible by increasing multivalent cation concentration, confirming the significant role of multivalent cations in oligonucleotide-directed triple-helix formation under these conditions. Finally, a small reduction in association rate, a large increase in dissociation rate, and a resulting reduction in the equilibrium binding constant were observed upon increasing the pH between 6.8 and 7.2.

The measurement of DNA reassociation kinetics has been employed to gain insight into both the interactions between charged polymers and the distribution of information in genomes. The fundamental characteristics of nucleic acid reassociation reactions may be summarized as follows [for reviews and theoretical considerations, see Marmur et al. (1963), Wetmur and Davidson (1968), Britten and Davidson (1985), and Young and Anderson (1985)]. Renaturation of denatured DNA exhibits a second-order dependence on DNA concentration, where the maximum rate of renaturation occurs at a temperature about 25 °C below the DNA melting transition temperature. Over the typical range of buffer conditions and nucleic acid lengths involved, the double-helical products of such reactions are completely stable. If one nucleic acid strand is in substantial excess over the other, the reaction kinetics are pseudo first order. The rate of renaturation at constant nucleotide concentration is increased by increasing DNA fragment length, increasing ionic strength, or increasing effective DNA concentration by addition of polymers and is decreased by increasing microscopic solvent viscosity. In this report, a hybridization kinetics approach is employed to analyze the rate of association of an oligodeoxyribonucleotide at a specific target site within a larger double-helical DNA polymer.

Pyrimidine oligodeoxyribonucleotide-directed triple-helix formation offers a method for the recognition of extended purine sequences in double-helical DNA (Moser & Dervan, 1987; Le Doan et al., 1987; Strobel et al., 1988; Praseuth et al., 1988; Lyamichev et al., 1988; Povsic & Dervan, 1989; Maher et al., 1989; Griffin & Dervan, 1989; Strobel & Dervan, 1989; Sun et al., 1989; Strobel & Dervan, 1990). The pyrimidine oligomer is oriented in the major groove of DNA parallel to the Watson–Crick purine strand (Moser & Dervan, 1987). Early studies of polymeric triple-helical nucleic acids suggested that specificity is imparted by Hoogsteen hydrogen-bonded base triplets, T·AT and C+GC (Felsenfeld et al., 1957; Hoogsteen, 1959; Lipsett, 1963; Howard et al., 1964; Michelson et al., 1967; Felsenfeld & Miles, 1967; Arnott & Selsing, 1974; Lee et al., 1979). Although no high-resolution X-ray structures of triple-helical DNA or RNA exist, two-dimensional nuclear magnetic resonance studies have confirmed the validity of these models (Rajagopal & Feigon, 1989; de los Santos et al., 1989). Near neutral pH and physiological temperature, existing methods based on Hoogsteen hydrogen bonding limit potential binding sites to purine sequences, although more generalized recognition may become feasible (Griffin & Dervan, 1989). Recognition of G-rich purine sequences appears to be possible with an alternative triple-helix motif based on purine hydrogen bonding to the purine strand (Cooney et al., 1988).

A series of previous experiments demonstrated that a local triple helix formed by the binding of oligopyrimidines to a 21-bp[1] purine sequence in a 6.4-kbp plasmid (37 °C, pH 6.8, 70 mM sodium chloride, 20 mM magnesium chloride, 0.4 mM spermine tetrahydrochloride) is stable for at least 2 h and blocks DNA recognition by sequence-specific DNA binding proteins such as restriction endonucleases (Maher et al., 1989).

† Supported by research grants from the National Institutes of Health (GM-35724) and the Beckman Institute of the California Institute of Technology and an American Cancer Society Postdoctoral Fellowship to L.J.M.

* To whom correspondence should be addressed.

[1] Abbreviations: bp, base pair; EDTA, ethylenediaminetetraacetic acid; nt, nucleotide; PIPES, 1,4-piperazinediethanesulfonic acid; SDS, sodium dodecyl sulfate; SEM, standard error of the mean; Tris, tris(hydroxymethyl)aminomethane.

0006-2960/90/0429-8820$02.50/0 © 1990 American Chemical Society

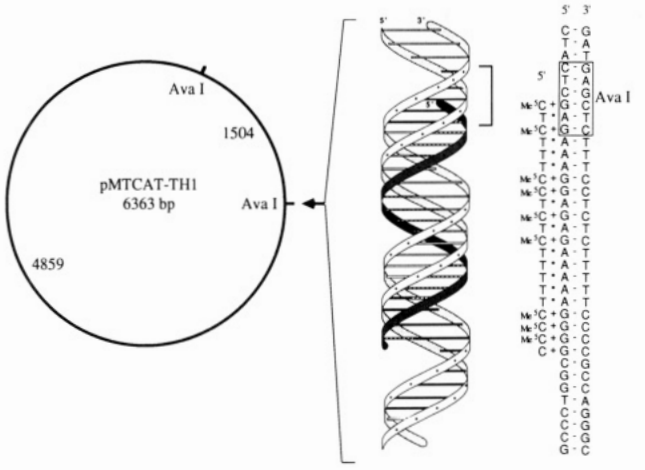

FIGURE 1: Restriction map of pMTCAT-TH1 and schematic representation of the triple-helical complex involving oligonucleotide **1**. Locations of *Ava*I recognition sites and the purine triple-helix target site (expanded region) are indicated. The *Ava*I recognition site overlapping the purine sequence is indicated by a bracket (center) and by a box (right). (−) indicates Watson–Crick base pairing, while (·) and (+) indicate Hoogsteen hydrogen bonds between adenine and thymine and between guanine and protonated cytosine, respectively. Oligonucleotide **1** is identical with oligonucleotide **4** previously described (Maher et al., 1989).

Of the oligonucleotides tested, a 21-nt oligopyrimidine containing 5-methylcytosine produced the most stable triple-helical complex at this site (Maher et al., 1989). Using this system, we now report experiments designed to examine the kinetics of oligodeoxyribonucleotide binding to, and dissociation from, double-helical DNA where the degree of endonuclease protection is a measure of complex formation over time. These studies provide useful insights into the role of kinetic parameters in oligonucleotide-directed triple-helix formation and stability. In addition, association and dissociation rates are examined under varying buffer conditions. There appear to be significant similarities and differences between oligonucleotide-directed triple-helix formation and the association of nucleic acid single strands. These results aid in the interpretation of previous experiments and will be valuable for design of future applications of double-helical DNA recognition by oligonucleotides or their analogues (Dervan, 1989, 1990).

Experimental Procedures

DNA. The construction of recombinant plasmid pMTCAT-TH1 has been described (Maher et al., 1989). This 6363-bp plasmid contains the mouse metallothionein I promoter modified by site-directed mutagenesis to contain a 21-bp purine sequence for pyrimidine oligonucleotide binding. Plasmid pMTCAT-TH1 also contains the chloramphenicol acetyltransferase coding sequence and SV40 splicing and polyadenylation signals. Supercoiled plasmid DNA was prepared by the alkaline lysis method (Maniatis et al., 1982) and was purified twice by banding in cesium chloride gradients in the presence of ethidium bromide. A simplified restriction map of plasmid pMTCAT-TH1 is shown in Figure 1. The oligonucleotide binding target is a 21-bp purine sequence that partially overlaps an *Ava*I restriction endonuclease recognition site. The resulting local triple-helical complex is also shown schematically in Figure 1. The sequence of oligonucleotide **1** is indicated. Oligonucleotides were prepared on a Beckman System 1Plus DNA synthesizer or an Applied Biosystems Model 380B DNA synthesizer with β-cyanoethyl phosphoramidites. Oligonucleotides were purified by denaturing polyacrylamide gel electrophoresis and were desalted by dialysis or by reverse-phase chromatography with Sep-Pak cartridges (Waters). The concentration of single-stranded oligonucleotides was determined at 260 nm, the following molar extinction coefficients ($M^{-1}\cdot cm^{-1}$) being used for each base (Moser & Dervan, 1987; Povsic & Dervan, 1989): 15400 (A), 11700 (G), 7300 (C), 5700 (Me^5C), and 8800 (T). Oligonucleotides were added to binding reactions as a concentrated aqueous solution.

Oligonucleotide Association Reactions. Binding reactions included supercoiled pMTCAT-TH1 DNA (1 or 10 nM) and association buffer. Association buffer, previously termed competition buffer (Maher et al., 1989), contains the following components (concentrations): Tris–acetate, pH 6.8 (25 mM), sodium chloride (70 mM), magnesium chloride (20 mM), spermine tetrahydrochloride (0.4 mM), β-mercaptoethanol (10 mM), and bovine serum albumin (0.1 mg/mL). Spermine tetrahydrochloride enhances triple-helix formation (Moser & Dervan, 1987). Buffer pH refers to the 10-fold-concentrated stock buffer solution at 22 °C. Buffer pH and concentrations of sodium chloride and magnesium chloride were varied in some experiments, as noted. For pH-variation experiments, Tris–acetate (25 mM) was employed for pH values of 7.2, 7.0, and 6.8; PIPES (25 mM) was employed for pH 6.0. Binding reactions were initiated by the addition of oligonucleotide (10 nM to 10 μM) and were incubated at 37 °C under paraffin oil in sealed tubes to prevent evaporation.

Oligonucleotide Dissociation Reactions. Oligonucleotide dissociation rates were measured by allowing oligonucleotides (100 nM) to incubate with supercoiled pMTCAT-TH1 DNA (10 nM) for 24 h at 37 °C in 50-μL reactions under paraffin oil. Incubation was performed either in standard association buffer or under modified conditions. Unbound oligonucleotides were separated from the triple-helical complexes by spun-column gel filtration chromatography with Sephadex G-75 (Pharmacia), essentially as described (Maniatis et al., 1982). Immediately after chromatography, the triple-helical complexes were incubated at 37 °C under paraffin oil. Samples (2.5 μL, 100 ng of plasmid) were removed at various times for restriction endonuclease analysis as described below.

AvaI Endonuclease Protection Assay. Samples of the association or dissociation reactions were removed at various times in order to analyze the extent of triple-helix formation. For reactions containing 1 nM pMTCAT-TH1 DNA, 25-μL samples were removed and analyzed as described below. For reactions containing 10 nM pMTCAT-TH1, 2.5-μL samples were removed and the buffer composition and volume adjusted so as to yield a final volume of 25 μL of association buffer. An *Ava*I endonuclease protection assay was used to measure the extent of triple-helix formation at the purine target site of supercoiled pMTCAT-TH1. This assay is based on the observation that, when bound to a purine site in a supercoiled plasmid, pyrimidine oligonucleotides protect an overlapping *Ava*I recognition sequence from digestion by *Ava*I (Maher et al., 1989). A distant *Ava*I site is not affected by oligonucleotide binding and serves as an internal control to rule out nonspecific inhibition of *Ava*I cleavage. *Ava*I endonuclease (10 units/μL) was obtained from Pharmacia or New England Biolabs. *Ava*I (10 units) was added to plasmid samples, and digestion was allowed to proceed at 37 °C for 10 min. In some cases, 20- or 40-min digestions were performed at lower enzyme concentrations. Digestions were terminated by the addition of agarose gel loading buffer (4 μL) containing TAE buffer (Maniatis et al., 1982), EDTA (100 mM), glycerol (56% v/v), SDS (0.2% w/v), and bromophenol blue (0.2

mg/mL). Half of each *Ava*I protection reaction (15 μL) was loaded into each lane of a 0.8% (w/v) agarose slab gel. Electrophoresis was performed at 2.7 V/cm for 2–4 h at 22 °C in TAE buffer containing 0.5 μg/mL ethidium bromide (Maniatis et al., 1982).

Quantitation. DNA was visualized by ethidium bromide fluorescence upon ultraviolet transillumination (254 nm). A photographic image was obtained by 1–2-min exposure (f4.5) of Polaroid type 55 positive/negative film at a distance of approximately 0.3 m in the presence of an orange filter. The resulting negative image was quantitated on an LKB Ultrascan XL scanning densitometer. Peak areas corresponding to the one, two, or three DNA bands in each lane were calculated by determining the mass of copies of the peak tracings with a microbalance. The extent of *Ava*I protection at the triple-helix site is reflected by the distribution of fluorescence between DNA fragments of 1504, 4859, and 6363 bp. The fractional *Ava*I protection (F) is defined as

$$F = A_{6363}/(A_{6363} + A_{4859} + A_{1504}) \quad (1)$$

where A_i is the area of peak i (i = 6363, 4859, or 1504). Thus, percent *Ava*I protection is given by $100F$. F is an experimental measure of θ, the fraction of double-helical target sites occupied by bound oligonucleotide.

Data Analysis. A nonlinear least-squares approach designed for analysis of RNA excess hybridization kinetics was used to analyze the association kinetic data (Pearson et al., 1977; Young & Anderson, 1985). The program was created to allow for a nucleic acid component that cannot associate, as well as for one or more components that associate according to pseudo-first-order rate equations of the form

$$B/B_0 = \exp[-(k_{2obs}R_0t)] \quad (2)$$

where B is the single-stranded probe DNA concentration (mol of nt·L^{-1}), R is the single-stranded RNA driver concentration [mol of nt·L^{-1}], t is time (s), k_{2obs} is the observed pseudo-first-order rate constant [L·(mol of nt)$^{-1}$·s^{-1}], and the subscript 0 indicates initial conditions. An identical procedure was applied to the kinetic analysis of oligonucleotide-directed triple-helix formation, where the oligonucleotide was maintained in substantial excess relative to the plasmid DNA target site. The corresponding pseudo-first-order rate equation is

$$D/D_0 = \exp[-(k_{2obs}O_0t)] \quad (3)$$

where D is the double-stranded DNA concentration (mol of nt·L^{-1}). Thus, D is the concentration of plasmid DNA containing an unoccupied triple-helix target site, and $D/D_0 = 1 - \theta$. O is the concentration of unbound oligonucleotide (mol of nt·L^{-1}). The applicability of this model to various experimental conditions is discussed under Results. For an oligonucleotide of length x, the molecule-based value for k_{2obs} [L·(mol of oligomer)$^{-1}$·s^{-1}] is x-fold greater than the value of k_{2obs} expressed as L·(mol of nt)$^{-1}$·s^{-1}. The curve-fitting procedure involved computer refinement of kinetic parameter estimates based on graphical data analysis.

Restriction endonuclease and restriction methylase protection experiments based on photographic detection of ethidium bromide fluorescence have been used qualitatively to demonstrate that triple-helical complexes are kinetically stable (Maher et al., 1989). Accurate quantitation of triple-helix formation using this photographic technique requires consideration of the relationship between actual fluorescent intensity and film response. A previous analysis has shown that film response is not a linear function of fluorescent intensity for DNA molecules of substantially different sizes (Pulleyblank et al., 1977). Care was therefore taken to verify that kinetic calculations using photographic parameters such as F (eq 1) were not strongly influenced by the shape of the film response curve.

Results

Oligonucleotide Association Kinetics. In previous experiments, plasmid DNA containing overlapping restriction and purine sites was challenged by the simultaneous addition of restriction endonuclease and oligonucleotide (Maher et al., 1989). Complete endonuclease protection under these experimental conditions required micromolar concentrations of oligonucleotides containing 5-methylcytosine. This requirement is expected to result from the concentration of oligonucleotides and the rate of triple-helix formation relative to the rate of the endonuclease binding and cleavage reaction. We now wish to dissect the parameters that govern the formation rate and stability of triple helices.

A reversible oligonucleotide binding reaction may be described by the following equilibrium expression:

$$D + O \underset{k_1}{\overset{k_{2pure}}{\rightleftharpoons}} T \quad (4)$$

where D, O, and T refer to double-helical target site, oligonucleotide, and triple-helical complex, respectively. Constants k_{2pure} and k_1 are the second-order association rate constant and first-order dissociation rate constant, respectively. In the presence of excess oligonucleotide relative to double-helical target site, the oligonucleotide concentration remains closely approximated by the initial oligonucleotide concentration, O_0. The kinetics for such a reaction are described by

$$\frac{D - D_{eq}}{D_0 - D_{eq}} = \exp[-(k_1 + k_{2pure}O_0)t] \quad (5)$$

where the subscripts 0 and eq refer to initial and equilibrium concentrations, respectively. Under conditions where the equilibrium described in eq 4 lies far to the right, the binding reaction is essentially irreversible, and eq 5 simplifies to a psuedo-first-order form (eq 3 under Experimental Procedures).

To assess the kinetics of oligonucleotide binding to pMTCAT-TH1, supercoiled plasmid DNA (1 nM) and various concentrations of oligonucleotides were mixed in association buffer and incubated at 37 °C. The extent of triple-helix formation at the purine target site of pMTCAT-TH1 was monitored at various times by subsequently challenging the plasmid DNA with *Ava*I restriction endonuclease (0.4 unit/μL final concentration). The results of such an experiment with oligonucleotide **1** are shown in Figure 2. The photographic negative obtained from panel A was quantitated by densitometry, and data points from the intermediate ranges of each curve are replotted in panel B against corresponding values of O_0t (expressed in mol of nt·s·L^{-1}). Horizontal error bars indicate the duration of the 10-min *Ava*I digestion reaction. Also plotted in panel B is the pseudo-first-order reaction curve fit to these data with eq 3. The value of the observed pseudo-first-order rate constant ± SEM obtained by analysis of four experiments of this type is 86 ± 9 L·(mol of nt)$^{-1}$·s^{-1}, equivalent to $1.8 \times 10^3 \pm 1.9 \times 10^2$ L·(mol of oligomer)$^{-1}$·s^{-1}. The results of similar experiments using oligonucleotides synthesized with cytosine rather than 5-methylcytosine indicated no detectable association rate at these concentrations (data not shown). This result is consistent with previous measurements of 5-methylcytosine enhancement of oligonucleotide binding (Maher et al., 1989).

Oligonucleotide Dissociation Rate. To determine the kinetic stability of the triple-helical complex, oligonucleotide disso-

Table I: Kinetic Parameters for Oligodeoxyribonucleotide-Directed Triple-Helix Formation under Various Conditions

	reaction conditions			
	standard	modifications		
parameter	70 mM NaCl, 20 mM $MgCl_2$, 400 μM spermine, pH 6.8	600 mM NaCl, 20 mM $MgCl_2$, 400 μM spermine, pH 6.8	70 mM NaCl, 20 mM $MgCl_2$, 400 μM spermine, pH 7.0	70 mM NaCl, 20 mM $MgCl_2$, 400 μM spermine, pH 7.2
k_{2obs} [L·(mol of oligomer)$^{-1}$·s^{-1}] × 10^{-3} [a]	1.8 ± 0.2	0.72 ± 0.05	2.5 ± 0.4	3.0 ± 0.9
k_1 (s^{-1}) × 10^5	2.2	16	10	24
complex half-life (s) × 10^{-4}	3.2	0.43	0.69	0.29
θ_{eq} [b]	0.91 ± 0.05	0.34 ± 0.06	0.63 ± 0.08	0.25 ± 0.03
k_{2pure} [L·(mol of oligomer)$^{-1}$·s^{-1}] × 10^{-3} [c]	2.2	0.82	1.7	0.8
K_{diss} (M) × 10^9 [d]	10	195	59	300

[a] Based on least-squares analysis of association rate curve. [b] Given by the fraction of double-helical target DNA sites in triple-helical form at equilibrium. [c] Calculated from $k_1\theta_{eq}\{[\text{oligomer}](1-\theta_{eq})\}^{-1}$. [d] Calculated from $k_1/k_{2pure} = [\text{oligomer}](1-\theta_{eq})/\theta_{eq}$.

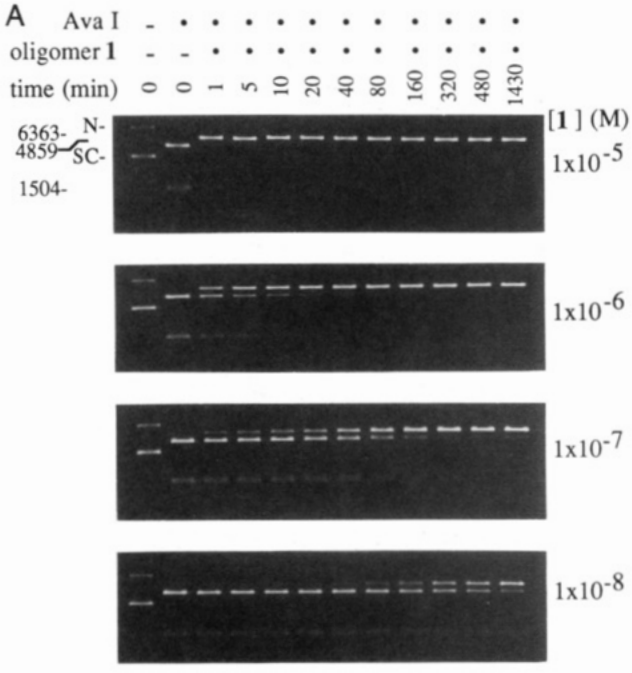

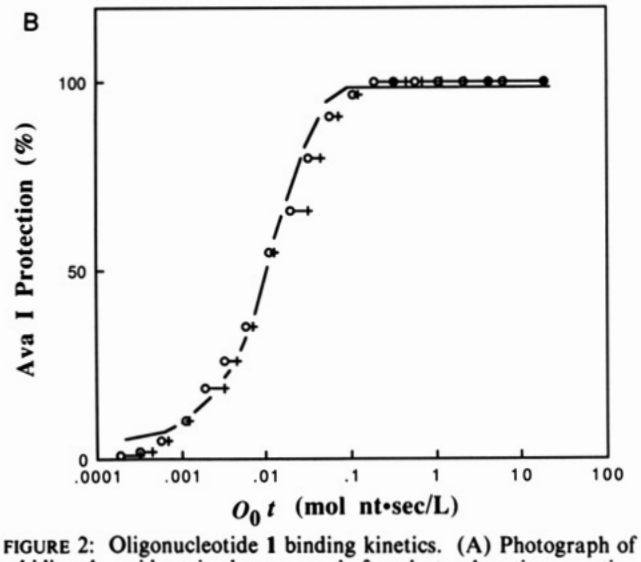

FIGURE 2: Oligonucleotide **1** binding kinetics. (A) Photograph of ethidium bromide stained agarose gel after electrophoretic separation of pMTCAT-TH1 fragments. Fragment lengths as well as nicked (N) and supercoiled (SC) plasmid mobilities are indicated at the left. The first lane of each row contains uncut plasmid DNA. The second lane contains plasmid DNA treated with *Ava*I in the absence of oligonucleotide. Oligonucleotide concentration (M) is indicated at the right. (B) O_0t plot of data from the intermediate range of each concentration set. Curve fitting was performed with the computer program described under Experimental Procedures. Horizontal error bars reflect the duration of the *Ava*I digestion reaction.

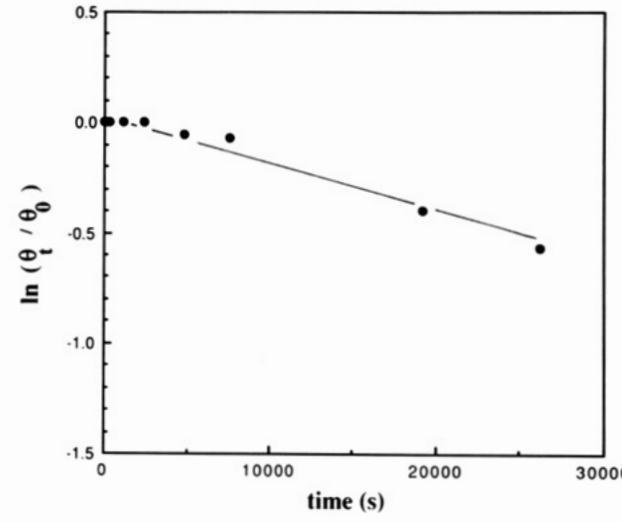

FIGURE 3: Oligonucleotide dissociation rates under standard conditions. Plasmid pMTCAT-TH1 (10 nM) was incubated for 24 h at 37 °C in the presence of oligonucleotide **1** (100 nM) in association buffer. Plasmid DNA was rapidly purified from unbound oligonucleotides as described under Experimental Procedures and incubated at 37 °C in association buffer. Decay of triple-helical complexes was monitored over time by *Ava*I endonuclease digestion. Subscripts 0 and t refer to values of θ (fraction of plasmid target sites in triple-helical form) at times 0 and t after removal of unbound oligonucleotides.

ciation rates were measured by removing unbound oligonucleotide **1** from the plasmid target and observing the rate of decay of the purified triple-helical complexes over time. Spun-column gel filtration chromatography proved to be a simple and rapid method for removing unbound oligonucleotides. As shown in Figure 3, plots of ln θ (the logarithm of the fraction of remaining triple-helical complex) versus time were linear, consistent with first-order dissociation kinetics. The measured value for the first-order dissociation rate constant, k_1, and the corresponding complex half-life are given in the second column of Table I for standard experimental conditions.

Cation Concentration Effects on Triple-Helix Formation. It has been well documented that the rate of reassociation of nucleic acid single strands is strongly enhanced by increasing sodium ion concentration at least up to 1.0 M (Wetmur & Davidson, 1968). The rate and extent of triple-helix formation directed by oligonucleotide **1** were examined in the presence of increasing sodium ion concentrations to determine if a similar relationship would be observed. Plasmid DNA (10 nM molecules) was incubated in the presence of oligonucleotide **1** (100 nM molecules) at 37 °C in association buffer containing increasing concentrations of sodium chloride. At various times, plasmid DNA (100 ng, 2.5 μL) was removed and diluted to

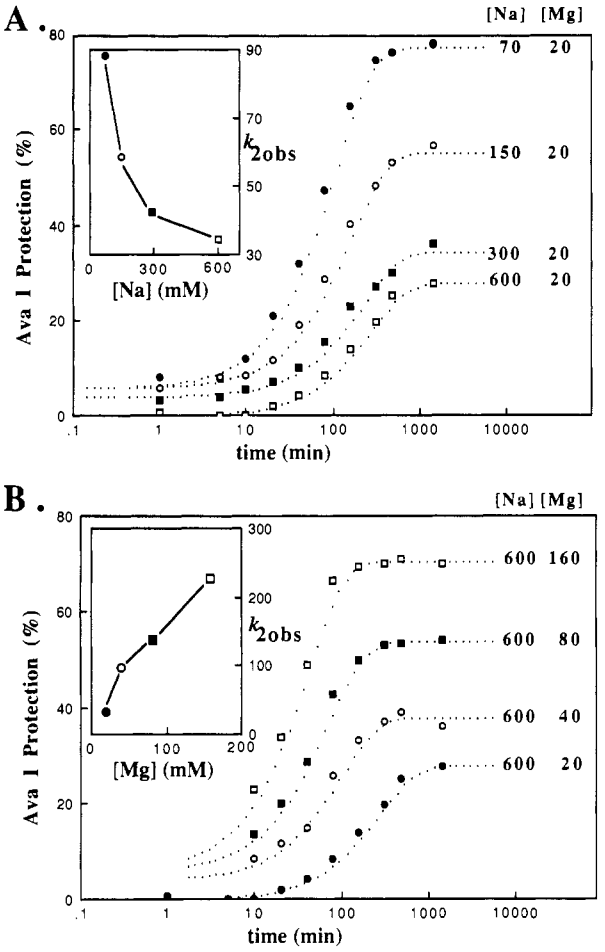

FIGURE 4: (A) Effect of sodium ion concentration on triple-helix formation. Plasmid pMTCAT-TH1 (10 nM molecules) was incubated at 37 °C in association buffer (●) or association buffer modified to include 150 (○), 300 (■), or 600 mM (□) sodium chloride and oligonucleotide **1** (100 nM molecules). Plasmid samples (100 ng) were removed at the indicated times, diluted, and treated with *Ava*I as described under Experimental Procedures. The inset displays the deduced effect of sodium ion concentration on the rate of triple-helix formation. The values of k_{2obs} are expressed in units of L·(mol of nt)$^{-1}$·s^{-1}. (B) Effect of magnesium ion concentration on triple-helix formation in the presence of 600 mM sodium chloride. Plasmid pMTCAT-TH1 (10 nM) was incubated at 37 °C in association buffer modified to include 600 mM sodium chloride and 20 (●), 40 (○), 80 (■), or 160 mM (□) magnesium chloride and oligonucleotide **1** (100 nM). Plasmid samples (100 ng) were removed at the indicated times, diluted, and treated with *Ava*I as described under Experimental Procedures. The inset displays the deduced effect of magnesium ion concentration on the rate of triple-helix formation under these conditions. The values of k_{2obs} are expressed in units of L·(mol of nt)$^{-1}$·s^{-1}.

a volume of 25 μL such that the final buffer concentration was equivalent to association buffer. Samples were then analyzed by *Ava*I digestion. In this and subsequent experiments, a nonlinear least-squares analysis based on eq 3 was performed to fit all binding curves. As described above, however, this model should be considered most accurate for reactions that approach completion at equilibrium. The result of this experiment is shown in Figure 4A. Remarkably, increasing sodium ion concentration from 70 to 600 mM caused an approximately 3-fold *decrease* in both the observed association rate and the extent of triple-helix formation, θ_{eq}.

To understand better this unexpected result, the sodium ion concentration was maintained at 600 mM (inhibitory concentration), and the concentration of magnesium ion was independently increased from 20 to 160 mM. The concentrations of the remaining association buffer components were held

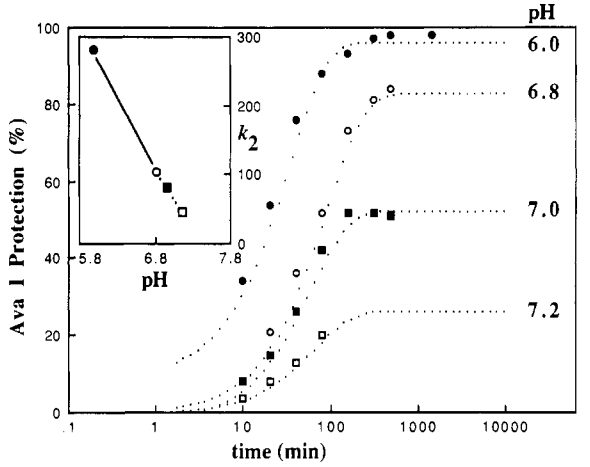

FIGURE 5: Effect of pH on extent and rate of triple-helix formation in association buffer. Plasmid pMTCAT-TH1 (10 nM) was incubated at 37 °C in association buffer modified to pH 6.0 (●), pH 6.8 (○), pH 7.0 (■), or pH 7.2 (□) and oligonucleotide **1** (100 nM). Plasmid samples (100 ng) were removed at the indicated times, diluted, and treated with *Ava*I as described under Experimental Procedures. The inset displays the deduced effect of pH on the rate of triple-helix formation under these conditions. The values of k_{2obs} (solid line) are expressed in units of L·(mol of nt)$^{-1}$·s^{-1}. Values of k_{2pure} (see Table I and Discussion) are indicated by dotted lines.

constant. The *Ava*I protection assay protocol was then repeated. The results of this experiment are shown in Figure 4B. Rather than continuing the trend observed for sodium ion, increasing magnesium ion in the presence of 600 mM sodium ion concentration *increased* both the rate and extent of triple-helix formation. The association rate increase was approximately 7-fold, while the extent of the reaction increased more than 2-fold. Thus, increasing concentrations of magnesium ion reverse the inhibitory effect of high sodium ion concentration on triple-helix formation.

pH Effects on Triple-Helix Formation. Previous experiments have demonstrated that neutral or acidic pH is required for triple-helix formation at purine sites in double-helical DNA by pyrimidine oligonucleotides containing cytosine (Moser & Dervan, 1987; Lyamichev et al., 1988). The dependence of Hoogsteen hydrogen bonding on protonation at N3 of cytosine appears to explain this observation. Substitution of 5-methylcytosine for cytosine in such oligonucleotides has been shown to extend the pH range compatible with complex formation (Povsic & Dervan, 1989). To examine the effect of pH on both the extent and rate of complex formation with the *Ava*I protection assay, an experiment was performed in association buffer at several pH values with pMTCAT-TH1 and oligonucleotide **1**. The results are shown in Figure 5. Consistent with previous results, increasing pH from 6.0 to 7.2 was observed to decrease the extent of triple-helix formation by more than 3-fold. Values of k_{2obs} (deduced from curve fitting with these data) or k_{2pure} (see Table I and Discussion) indicate that the rate of triple-helix formation is also substantially decreased over this pH interval.

Effects of pH and Sodium Ion Concentration on Oligonucleotide Dissociation Rates. Under certain conditions (increased pH, increasing sodium ion concentration), the apparent equilibrium value of θ (fraction of plasmid target site converted to triple helix) at kinetic termination was found to be significantly less than unity. This observation suggested that the equilibrium dissociation constant for the intermolecular triple helix was increased in these cases. Dissociation rate constants were measured under several conditions. The results are shown in Figure 6 and Table I. Addition of 600

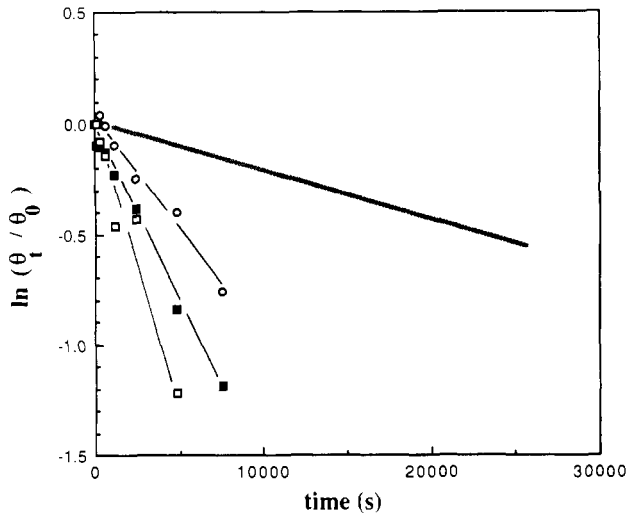

FIGURE 6: Oligonucleotide dissociation rates under nonstandard conditions. Plasmid pMTCAT-TH1 (10 nM) was incubated for 24 h at 37 °C in the presence of oligonucleotide **1** (100 nM) under various conditions. Plasmid DNA was rapidly purified from unbound oligonucleotides as described under Experimental Procedures and incubated at 37 °C under appropriate conditions. Decay of triple-helical complexes was monitored over time by *Aval* endonuclease digestion. Subscripts 0 and t refer to values of θ (fraction of plasmid target sites in triple-helical form) at times 0 and t after removal of unbound oligonucleotides. Reaction conditions are as follows: association buffer (shaded line); association buffer containing 600 mM sodium chloride (■); association buffer at pH 7.0 (○); association buffer at pH 7.2 (□).

mM sodium chloride to standard association buffer increased the dissociation rate 7.5-fold. Increasing pH to 7.0 or 7.2 increased the dissociation rate 4- and 12.5-fold, respectively. Thus, changes in dissociation rate account for most of the retardation in observed association rate. Moreover, the increased rate of dissociation results in an increased K_{diss} at higher pH and higher sodium ion concentration. This effect is reflected in the decreased value for θ_{eq}, the fraction of double-helical target site in triple-helical form at equilibrium.

Discussion

The kinetics of site-specific oligonucleotide binding to double-helical DNA have been analyzed with a restriction endonuclease protection assay. In the presence of greater than 10-fold excess pyrimidine oligonucleotide **1** relative to the pMTCAT-TH1 target site, the kinetics of oligonucleotide association with the plasmid are approximately pseudo first order in oligonucleotide concentration (37 °C, 25 mM Tris–acetate, pH 6.8, 70 mM sodium chloride, 20 mM magnesium chloride, 0.4 mM spermine tetrahydrochloride, 10 mM β-mercaptoethanol, 0.1 mg/mL bovine serum albumin). The calculated value for the observed forward rate constant, k_{2obs}, is $1.8 \times 10^3 \pm 1.9 \times 10^2$ L·(mol of oligomer)$^{-1}$·s^{-1}.

It would be of interest to compare the rate of oligonucleotide binding to double-helical DNA with the rate of oligonucleotide binding to a single-stranded target site. A direct comparison of this type is presently made difficult because reaction rates observed under the conditions of multivalent cations, oligonucleotide length, and temperature used in these experiments cannot readily be corrected to the corresponding rates for standard hybridization kinetic measurements. In any case, it is important to recognize that association rates between oligonucleotides and single- or double-stranded structures may be limited by different factors. For example, there is substantial evidence that competing intramolecular base pairing can dramatically slow the association of complementary strands (Studier, 1969; Straus & Bonner, 1972; Gamper et al., 1987). Similarly, the rate of oligonucleotide-directed triple-helix formation might be reduced if intra- or intermolecular oligonucleotide base-pairing interactions arise. However, in contrast to annealing of complementary single strands, availability of the double-helical DNA target itself is not generally expected to be limited by alternative secondary structures.

The value of k_{2obs} provides insight into the requirement for substantially higher concentrations of oligonucleotide **1** when the protection assay is performed as originally described (Maher et al., 1989). In that case, *Aval* endonuclease was added without prior equilibration of oligonucleotide and target plasmid. In this direct competition for overlapping binding sites, endonuclease protection required that the forward reaction rate be greater than the association rate of *Aval*. The necessary rate increase was provided by additional oligonucleotide concentration. As shown by the results reported here, substantially lower oligonucleotide concentrations are required for *Aval* protection if a preliminary oligonucleotide binding reaction is performed. Whereas 50% endonuclease protection required 250 nM oligonucleotide **1** in the absence of a preliminary binding reaction (Maher et al., 1989), comparable endonuclease protection is obtained with 10 nM oligonucleotide **1** after a 24-h binding reaction (a 25-fold reduction).

The observed similarity between the kinetics of oligonucleotide-directed triple-helix formation and RNA excess hybridization prompted an examination of the rate effect of increasing ionic strength (sodium chloride concentration). Single-strand hybridization rates are known to be significantly increased by increasing monovalent cation concentration under conditions of total ionic strength similar to those studied here (Wetmur & Davidson, 1968; Studier, 1969). Figure 4A shows that, in contrast to the results expected by analogy with the annealing of complementary single strands, increasing sodium chloride concentration from 70 to 600 mM substantially decreases the extent of triple-helix formation, predominantly by increasing oligonucleotide dissociation rate. This result seems more consistent with the known effect of monovalent cations on DNA binding by multivalent cations (Manning, 1978; Record et al., 1978). This suggests that the binding of multivalent cations may play a critical role in triple-helix formation under our experimental conditions. Further evidence in support of this proposition comes from the data shown in Figure 4B. In these experiments, the total ionic strength of buffers containing 600 mM sodium chloride was further increased by addition of magnesium chloride. Increasing the concentration of this divalent cation was sufficient to reverse, at least partially, the decreased association rate and extent induced by sodium ion. A more detailed understanding of the role(s) played by multivalent cations in triple-helix formation will require further studies.

The observed effect of pH on the extent of triple-helix formation appears consistent with the requirement for protonation of cytosine or 5-methylcytosine residues in the bound oligonucleotide (Rajagopal & Feigon, 1989; de los Santos et al., 1989). Theoretical calculations have been presented by others to suggest that the lifetimes of triple-helical complexes of this type should be exquisitely sensitive to changes in pH (Lyamichev et al., 1988). As shown in Table I, estimation of triple-helix complex half-lives between pH 6.8 and pH 7.2 does indicate substantial destabilization with increasing pH (approximately 13-fold decrease in half-life).

The data presented in Table I show that changes in reaction conditions such as increasing sodium ion concentration or

increasing pH tend to modestly decrease association rates and significantly increase dissociation rates, thus substantially changing the equilibrium constant for triple-helix formation. The reversibility of oligonucleotide binding reactions under these conditions makes them distinct from traditional reassociation reactions involving relatively long single-stranded polymers. In the latter case, changes in reaction conditions that affect association rates (ionic strength, temperature, etc.) usually do not prevent completion of the reassociation reaction.

The observation that triple-helical fibers diffract in an A-like configuration raises the possibility that a structural isomerization between B-form and A-form within the purine target sequence might control oligonucleotide association and dissociation rates (Arnott & Selsing, 1974). The experimental results reported here may be relevant to this issue. Throughout the range of oligonucleotide concentration studied (10 nM to 10 μM), the association reaction appears to be pseudo first order. If a B- to A-form isomerization in at least part of the double-helical DNA target sequence were required for nucleation of triple-helix formation, it might be expected that the isomerization event would become rate limiting at high oligonucleotide concentration. Achievement of a maximum association rate independent of oligonucleotide concentration was not observed over the range tested in this study.

The experiments reported here provide new insights into pyrimidine oligonucleotide binding to purine sequences in double-helical DNA. The reported measurements of association kinetics, cation, pH, and dissociation kinetics highlight critical parameters that must be considered in the application of oligonucleotide recognition of double-helical DNA to the specific cleavage of chromosomes (Strobel & Dervan, 1990) or the disruption of DNA–protein interactions (Maher et al., 1989). Of interest in this regard is the value of the oligonucleotide dissociation constant observed in these experiments. It may be biologically significant that the measured affinity of a highly anionic oligodeoxyribonucleotide for double-helical DNA (K_{diss} = 10 nM) approaches that observed for many sequence-specific DNA binding proteins. Furthermore, when associated with double-helical DNA near physiological pH and ionic conditions, the bound oligonucleotide has a half-life of approximately 12 h. These observations suggest that promoter-specific oligonucleotides or their analogues might effectively and specifically bind target DNA sequences in vivo. Such binding might affect gene expression by competing with sequence-specific DNA binding proteins, directing the binding of a protein–oligonucleotide complex, or altering higher order DNA structure.

Acknowledgments

We thank Jim Moore and Scott Singleton for assistance in data analysis and Dr. Norman Davidson for critical comments.

Registry No. 1, 123625-78-5; Na, 7440-23-5; Mg, 7439-95-4.

References

Arnott, S., & Selsing, E. (1974) *J. Mol. Biol. 88*, 509.

Britten, R. J., & Davidson, E. H. (1985) in *Nucleic Acid Hybridization* (Hames, B. D., & Higgins, S. J., Eds.) pp 3–15, IRL Press, Washington, DC.

Cooney, M., Czernuszewicz, G., Postel, E. H., Flint, S. J., & Hogan, M. E. (1988) *Science 241*, 456.

de los Santos, C., Rosen, M., & Patel, D. (1989) *Biochemistry 28*, 7282.

Dervan, P. B. (1989) in *Oligodeoxynucleotides, Antisense Inhibitors of Gene Expression* (Cohen, J. S., Ed.) pp 197–210, Macmillan Press, Ltd., London.

Dervan, P. B. (1990) in *Human Genome Initiative and DNA Recombination* (Sarma, R. H., & Sarma, M. H., Eds.) pp 37–49, Adenine Press, Guilderland, NY.

Felsenfeld, G., & Miles, H. T. (1967) *Annu. Rev. Biochem. 239*, 1256.

Felsenfeld, G., Davies, D. R., & Rich, A. (1957) *J. Am. Chem. Soc. 79*, 2023.

Gamper, H. B., Cimino, G. D., & Hearst, J. E. (1987) *J. Mol. Biol. 197*, 349.

Griffin, L. C., & Dervan, P. B. (1989) *Science 245*, 967.

Hoogsteen, K. (1959) *Acta Crystallogr. 12*, 822.

Howard, F. B., Frazier, J., Lipsett, M. N., & Miles, H. T. (1964) *Biophys. Biochem. Res. Commun. 17*, 93.

Le Doan, T., Perrouault, L., Praseuth, D., Habhoub, N., Decout, J.-L., Thuong, N. T., Lhomme, J., & Hélène, C. (1987) *Nucleic Acids Res. 15*, 7749.

Lee, J. S., Johnson, D. A., & Morgan, A. R. (1979) *Nucleic Acids Res. 6*, 3073.

Lipsett, M. N. (1963) *Biophys. Res. Commun. 11*, 224.

Lyamichev, V. I., Mirkin, S. M., Frank-Kamenetskii, M. D., & Cantor, C. R. (1988) *Nucleic Acids Res. 16*, 2165.

Maher, L. J., Wold, B., & Dervan, P. B. (1989) *Science 245*, 725.

Maniatis, T., Fritsch, E. F., & Sambrook, T. (1982) in *Molecular Cloning, A Laboratory Manual*, Cold Spring Harbor Laboratory, Cold Spring Harbor, NY.

Manning, G. S. (1978) *Q. Rev. Biophys. 11*, 179.

Marmur, J., Rownd, R., & Schildkraut, C. L. (1963) in *Progress in Nucleic Acid Research* (Davidson, J. N., & Cohn, W. E., Eds.) Academic Press, New York.

Michelson, A. M., Massoulié, J., & Guschlbauer, W. (1967) *Prog. Nucleic Acid Res. Mol. Biol. 6*, 83.

Moser, H. E., & Dervan, P. B. (1987) *Science 238*, 645.

Pearson, W. R., Davidson, E. H., & Britten, R. J. (1977) *Nucleic Acids Res. 4*, 1727.

Povsic, T. J., & Dervan, P. B. (1989) *J. Am. Chem. Soc. 111*, 3059.

Praseuth, D., Perrouault, L., Le Doan, T., Chassignol, M., Thuong, N., & Hélène, C. (1988) *Proc. Natl. Acad. Sci. U.S.A. 85*, 1349.

Pulleyblank, D. E., Shure, M., & Vinograd, J. (1977) *Nucleic Acids Res. 4*, 1409.

Rajagopal, P., & Feigon, J. (1989) *Nature 239*, 637.

Record, M. T., Anderson, C. F., & Lohman, T. M. (1978) *Q. Rev. Biophys. 11*, 103.

Straus, N. A., & Bonner, T. I. (1972) *Biochim. Biophys. Acta 277*, 87.

Strobel, S. A., & Dervan, P. B. (1989) *J. Am. Chem. Soc. 111*, 7286.

Strobel, S. A., & Dervan, P. B. (1990) *Science 249*, 73.

Strobel, S. A., Moser, H. E., & Dervan, P. B. (1988) *J. Am. Chem. Soc. 110*, 7927.

Studier, F. W. (1969) *J. Mol. Biol. 41*, 199.

Sun, J.-S., François, J.-C., Montenay-Garestier, T., Saison-Behmoras, T., Roig, V., Thuong, N. T., & Hélène, C. (1989) *Proc. Natl. Acad. Sci. U.S.A. 86*, 9198.

Wetmur, J. G., & Davidson, N. (1968) *J. Mol. Biol. 31*, 349.

Young, B. D., & Anderson, M. L. M. (1985) in *Nucleic Acid Hybridization* (Hames, B. D., & Higgins, S. J., Eds.) pp 3–15, IRL Press, Washington, DC.